INFECTION AND IMMUNITY, Jan. 2006, p. 663–672 Vol. 74, No. 1
0019-9567/06/$08.00+0 doi:10.1128/IAI.74.1.663–672.2006

Invasion of the Placenta during Murine Listeriosis

Alban Le Monnier,[1,2,3] Olivier F. Join-Lambert,[1,2,3] Francis Jaubert,[1,3,4] Patrick Berche,[1,2,3] and Samer Kayal[1,2,3]*

Faculté de Médecine, Université René Descartes Paris-5, U-570 INSERM, 156 rue de Vaugirard, 75730 Paris Cedex 15,[1] INSERM Paris,[2] and Assistance Publique-Hôpitaux de Paris,[3] Paris, and Département d'Anatomie Pathologique, Hôpital Necker-Enfants Malades, 149 rue de Sèvres, 75015 Paris,[4] France

Received 27 July 2005/Returned for modification 1 September 2005/Accepted 2 October 2005

Feto-placental infections due to *Listeria monocytogenes* represent a major threat during pregnancy, and the underlying mechanisms of placental invasion remain poorly understood. Here we used a murine model of listeriosis (pregnant mice, infected at day 14 of gestation) to investigate how this pathogen invades and grows within the placenta to ultimately infect the fetus. When *L. monocytogenes* is injected intravenously, the invasion of the placenta occurs early after the initial bacteremia, allowing the placental growth of the bacteria, which is an absolute requirement for vertical transmission to the fetus. Kinetically, bacteria first target the cells lining the central arterial canal of the placenta, which stain positively with cytokeratin, demonstrating their fetal trophoblast origin. Bacteria then disseminate rapidly to the other trophoblastic structures, like syncytiotrophoblast cells lining the villous core in the labyrinthine zone of placenta. Additionally, we found that an inflammatory reaction predominantly constituted of polymorphonuclear cells occurs in the villous placenta and participates in the control of infection. Altogether, our results suggest that the infection of murine placenta is dependent, at the early phase, on circulating bacteria and their interaction with endovascular trophoblastic cells. Subsequently, the bacteria spread to the other trophoblastic cells before crossing the placental barrier.

Listeria monocytogenes is a gram-positive bacterium widely spread in nature. As a facultative intracellular food-borne pathogen, it is responsible for both severe central nervous system and fetal infections in humans and in a large variety of animals (18). Although human listeriosis occurs anytime during pregnancy, it is frequently detected during the third trimester, resulting in intrauterine fetal death, abortion, preterm birth, or a neonatal infection with a severe septic syndrome known as granulomatosis infantiseptica. The placenta is a dynamic organ consisting of maternal and fetal tissues, forming an impermeable physical and biological barrier that protects the fetus against pathogens (8, 9, 24, 27, 42). Only a few intracellular pathogens can cross this barrier. This includes some viruses such as cytomegalovirus, parvovirus B19, or rubella (25), parasites such as *Toxoplasma gondii* (1, 8, 31), and rare bacteria such as *Brucella abortus* (35), *Chlamydia psittaci* (12, 22), *Coxiella burnetii* (44), and *L. monocytogenes* (10, 43). However, almost nothing is known about the molecular mechanisms responsible for the vertical transmission of pathogens across the feto-placental barrier. Several authors have reported the in vitro susceptibility of trophoblastic cells to pathogen infection (1, 20, 28, 30).

It is well established that the virulence of *L. monocytogenes* is due to its capacity to survive and multiply inside cells of infected hosts. The molecular basis of its intracellular parasitism has been elucidated to a large extent (review in reference 46). During infection, bacteria can proliferate within a variety of cells, including macrophages. Experimental listeriosis has been extensively studied in animals, but there are few reports of experimental placental listeriosis. Although feto-placental listeriosis has been induced in sheep (33) and recently in guinea pigs (6), most reports have used the murine model after intravenous inoculation. Under these conditions, feto-placental infection can be easily reproduced in pregnant mice (2, 3, 20, 30, 31, 37). This experimental murine model presents several advantages for studying the pathogenesis of listeriosis, including the availability of many immunological and genetic tools. In addition, recent studies provide extensive new data on the anatomy and the physiology of the mouse placenta (4, 15, 41). Despite some aspects unique to rodents, notably the blood circulation (4), mouse placenta is comparable to that of humans in that both are hemochorial placentas (9, 24, 41). It is known that the fetal-embryonic trophoblast cells play a central role in the development and the physiology of the placenta, including the establishment of local immunotolerance (20, 38). This structure also expresses an area of high phagocytic activity (5). In contrast to human placenta, the murine placenta displays some specific features (4), like spiral arteries which are prolonged by central arterial channels sending blood towards the opposite chorionic plate, as recently confirmed by a dynamic study of blood circulation (42). Interestingly, it has been shown that the wall of these central arterial channels is lined by trophoblastic cells that replace endothelial cells at the level of the proximal decidua basalis (4).

In the present work, we studied the invasion of placenta in pregnant mice intravenously infected by a virulent strain of *L. monocytogenes*. The kinetics of placental and fetal infection was monitored, and the requirement of an inflammatory response in the placenta, for the protection of the fetus, was determined.

* Corresponding author. Mailing address: INSERM U-570, Faculté de Médecine 156 rue de Vaugirard, 75730 Paris Cedex 15, France. Phone: 33-1-40-61-55-93. Fax: 33-1-40-61-55-92. E-mail: kayal@necker.fr.

MATERIALS AND METHODS

Bacterial strains and cultures. We used the sequenced wild-type virulent strain of *L. monocytogenes* serotype 1/2a (EGD). Bacteria were grown overnight

in brain heart infusion (BHI) broth (Difco Laboratories, Detroit, Mich.) at 37°C without antibiotics, collected at the end of the exponential phase, centrifuged at 5,000 × *g* for 20 min at 4°C, washed twice, suspended in RPMI-1640 medium (Difco), and stored at −80°C in 1-ml aliquots. Bacteria were titrated by serial dilution and plated on BHI agar. Before each experiment, an aliquot was thawed and diluted to obtain the appropriate cell suspension.

Mice. Inbred BALB/c gestating mice were purchased from Elevage Janvier (Le Genest-St-Isle, France). Couplings were carried out on 8- to 10-week-old BALB/c female mice. Mating was assessed by the appearance of a vaginal plug which denotes the first embryonic day of pregnancy. The gestation was checked at the 12th day, and nonpregnant females served as "non pregnant" control mice. Mice were housed in wire-bottom cages, with free access to food and water, and held in these conditions at least 24 h before infection. Animal experimentations were approved by the Animal Welfare Committee of the University Descartes-Paris 5 (Paris, France).

Infection of mice. BALB/c female mice were injected intravenously (i.v.) at the 14th day of gestation via the lateral tail vein with 0.5 ml of a calibrated suspension of *L. monocytogenes* (extemporaneously obtained by appropriate dilution into saline isotonic solution from a frozen stock). All animals were examined daily. At intervals after infection (6, 24, 48, and 72 h), groups of mice were anesthetized by intramuscular injection of 200 μl of a mixture of ketamine (200 mg kg^{-1}) (Imalgène 100; Merial, Lyon, France) and xylazine hydrochloride (10 mg kg^{-1}) (Rampun; Bayer, Puteaux, France) and were sacrificed. The abdominal cavity was then aseptically opened, and each mouse was bled by intracardiac puncture with a previously heparinized syringe (heparin sodic; Sanofi, Wintrop, France). Organs (livers, spleens, and brains) and each feto-placental unit were aseptically removed and homogenized for bacterial counts and histological studies. Each placenta and its respective fetus were independently dissected and analyzed. Bacterial counts were determined by plating serial 10-fold dilutions of each organ homogenate on BHI agar plates incubated at 37°C for 24 to 48 h. For each mouse, 100 μl of each placenta or fetus homogenate was separately pooled to determine the mean bacterial load. The results were expressed as a mean ± standard error expressed as $\log_{10}$ CFU per organ (bacteria/organ).

Depletion of mice PMNs with monoclonal antibody. We used a monoclonal antibody (MAb) produced by the hybridoma RB6-8C5 (a generous gift from Sophie Ezine, Paris, France) known to induce depletion of mouse polymorphonuclear cells (PMNs) and eosinophils (13, 45). The MAb RB6-8C5 was given by the peritoneal route in a dose of 250 μg in 200 μl, 1 day and 4 h before i.v. inoculation of 5×10^3 *L. monocytogenes* organisms. Control mice received, by the peritoneal route, 250 μg of rat immunoglobulin G (IgG) diluted in saline isotonic solution. White cell counts were performed by using a Sysmex XE2100 (Roche Diagnostics, Meylan, France) at various times on blood samples collected by intracardiac puncture. Leukocyte counts were controlled on May-Grunwald-Giemsa staining smears and examined under light microscopy (Nikon Eclipse E600 and a digital camera DXM1200).

The depletion induced by the MAb RB6-8C5 was verified by flow cytometry in the hematopoietic tissues of the mother (bone marrow) and the fetus (fetal liver). We used several antibodies against mouse antigens: anti-Ly6C/Ly6G (1:200; clone RB6-8C5) and anti-Ly6G (1:200; clone 1A8) phycoerythrin (PE) conjugates as well as anti-CD45 (1:800; clone 30-F11) biotin conjugate and anti-CD16/CD32 Fc-receptor (1:100; clone 2.4G2), all from Pharmingen (San Diego, CA). Maternal bone marrow was collected aseptically from femurs by flushing with 1 ml phosphate-buffered saline (PBS) containing 1% fetal calf serum (FCS) and refrigerated on ice. Bone marrow fragments were dissociated by pipetting up and down, centrifuged at 800 rpm for 5 min at 4°C, and resuspended in ice-cold PBS–1% FCS to a final concentration of 1×10^7 nucleated cells per ml. Fetal livers were collected, dissociated, and digested with collagenase D (solution at 1 mg/ml) (Roche Diagnostics) for 20 min at 37°C. Red blood cells were lysed by hypotonic shock with potassium ammonium chloride buffer for 5 min at room temperature. Cells were washed twice with ice-cold PBS–1% FCS and fixed in ice-cold 1.5% fresh paraformaldehyde solution for 10 min. After fixation, cells were washed in PBS–1% FCS and incubated with an anti-CD16/CD32 Fc-receptor MAb to block Fc-mediated antibody binding. Relevant antibodies were then incubated with cells for 30 min and subsequently washed twice with PBS–1% FCS. For CD45 labeling, cells were incubated with streptavidin Cychrome conjugate (1:1,600; Pharmingen, San Diego, CA). Cells were subsequently washed twice with PBS before analysis was performed by FACScan cytofluorography (Becton Dickinson, San Diego, CA). Data were analyzed using CellQuest software (Becton Dickinson).

Histology. Histological studies were performed on placenta removed from mice at intervals between days 15 and 17 of gestation after i.v. infection with 2×10^5 bacteria. Feto-placental units were removed from the uterus corns by dissociation between implantation sites. Placentas were separated from the fetuses. Half of each placenta was used to quantify bacterial load, and the other half was used for histological analysis. For light microscopy studies (Nikon Eclipse E600 and a digital camera DXM1200), placentas were fixed overnight in 10% formalin, dehydrated with an alcohol gradient, and embedded in paraffin blocks. Inclusions of placental sequential 5- to 7-μm sections were stained with hematoxylin-eosin or Gram-Weigert techniques. Additional semithin sections (0.2 μm) were processed from the same infected or noninfected placenta and fixed in 2.5% glutaraldehyde and 2% paraformaldehyde (Sigma Chemical Co., St. Louis, MO) in 0.1 M cacodylate buffer (pH 7.3) containing 0.1 M sucrose, 5 mM $CaCl_2$, and 5 mM $MgCl_2$ for 2 h. Samples were postfixed in 2% aqueous osmium tetroxide (Merck, Darmstadt, Germany) for 1 h, dehydrated in a series of graded alcohol solutions, and embedded in Epon 812 (Janning, Vanves, France). Semithin sections of placenta were prepared on glass slides and counterstained with toluidine blue and examined by light microscopy (Nikon Eclipse E600 and a digital camera DXM1200).

Serial sections from infected placentas embedded in paraffin blocks were previously treated to uncover the antigenic sites and to inhibit endogenous peroxidase by H_2O_2-CH_3OH (1% dilution) (Merck). They were then processed for immunohistochemistry to label cytokeratin (Z0622; polyclonal antibody [PAb] rabbit anti-keratin with spectrum screening, 1:200; Dako Diagnostics) of trophoblast cells, CD45 (553077; PAb biotin conjugates of rat anti-mouse, 1:100; BD Pharmingen, San Diego, CA) for leukocyte populations, or F4/80 (MCA 4976A; rat anti-mouse, 1:10; Serotec) for monocyte populations. For revealing antibody reactivity, we used an indirect method with secondary antibodies PAb swine anti-rabbit horseradish peroxidase (P0217; Dako) coupled with a Dako EnVison system for visualization (anti-rabbit K4010-labeled polymer horseradish peroxidase) or rabbit anti-rat peroxidase conjugate (A5795; Sigma) and diaminobenzidine (K3465; Dako).

Statistical analysis. All values are given as means ± standard errors. We compared the mean values by using multifactorial analysis of variance, and differences were considered significant for $P \leq 0.05$. Placentas and fetuses were considered infected when bacterial counts were superior or equal to 1 bacterium/placenta or to 50 bacteria/fetus. We used several statistical methods to determine the relationship between placental infection and the corresponding fetal infection. Receiver-operator characteristics analysis was used to identify the cutoff values for placental bacterial load associated with the maximal probability of fetal infection. We considered the following values: true-positive (TP) value was higher than cutoff when fetal infection was observed; true-negative (TN) value was lower than cutoff when fetal infection was not observed; false-negative (FN) value was lower than cutoff when fetal infection was observed; and false-positive (FP) value was higher than cutoff when no fetal infection was observed. Sensitivity (Se), specificity (Sp), positive predicted value (PPV), and negative predicted value (NPV) were calculated as follows: Se = TP/(TP + FN); Sp = TN/(FP + TN); PPV = TP/(TP + FP); and NPV = TN/(FN + TN). The selected cutoff value was associated with the highest combination of sensitivity and specificity.

RESULTS

Feto-placental infection during murine listeriosis. Pregnant BALB/c mice (day 14 of gestation) were injected i.v. with increasing doses of wild-type *L. monocytogenes* EGD strain (5×10^3, 5×10^4, and 5×10^5 bacteria per mouse). The kinetics of bacterial growth were then followed in the blood, the organs (liver, spleen, and brain), and in all the feto-placental units for 3 days. As illustrated in Fig. 1A, we found rapid bacterial growth in organs, depending upon the number of inoculated bacteria. No difference in bacterial growth in organs was observed between nonpregnant and pregnant mice (data not shown), suggesting that the infectious process is not altered by pregnancy during the early stages. The feto-placental infection of pregnant mice was followed by separating each fetus from its placenta. Individual data from placenta and fetus are plotted at indicated times in Fig. 1B (left panel), together with the logarithmic means (± standard error) and the corresponding percentages of infected placenta and fetus (right panel). We occasionally observed resorptions of feto-placental units in the uterus. We systematically controlled bacterial counts of the resorptions, and we never observed any infection. Thus, these

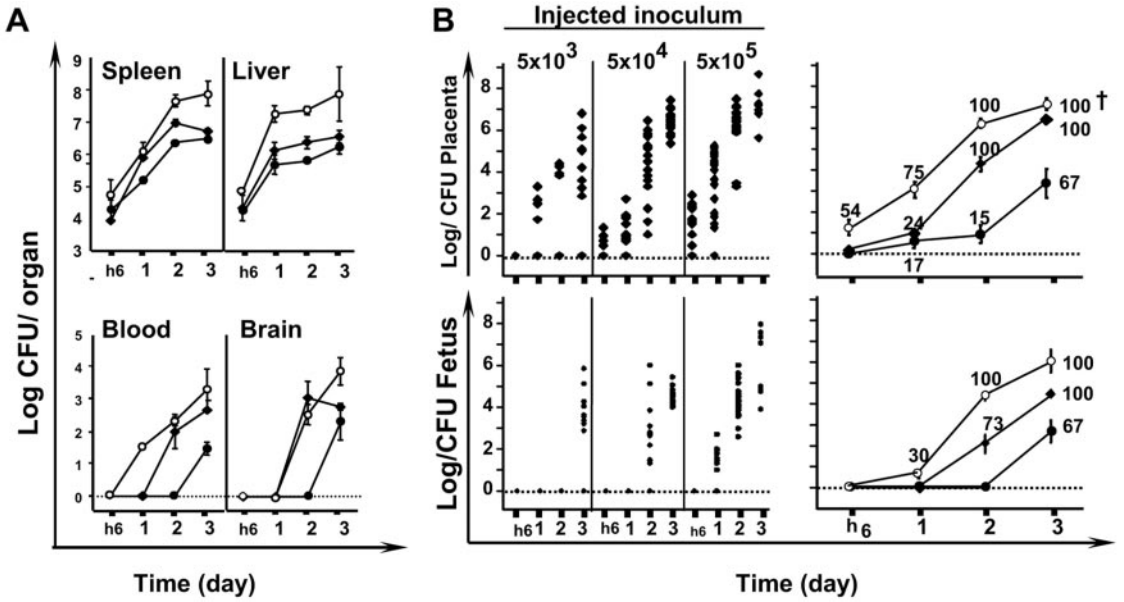

FIG. 1. *L. monocytogenes* (EGD) infection of pregnant BALB/c mice. Mice were injected intravenously at day 14 of pregnancy with different bacterial inocula (5×10^3 [○], 5×10^4 [◆], and 5×10^5 [●] bacteria). Animals were monitored by quantifying bacterial growth at the indicated times and inoculum. (A) Bacterial growth in organs (spleen, liver, and brain) and in blood of pregnant mice. Results shown are the means ± standard errors from groups of 3 to 5 mice (average litter size, 6.6 ± 1.5 placenta; range, 3 to 10) and are expressed as the $\log_{10}$ CFU/organ or $\log_{10}$/milliliter for the blood. (B) The kinetics of bacterial growth are represented on the left panels by dot plots corresponding to individual bacterial counts for each placenta (top panel) and each fetus (lower panel) for the indicated time and inoculum. In the right panels the means ± standard errors for each time and inoculum data are given. The number reported near each value corresponds to the percentage of infected placenta among all analyzed placentas. (Fetal loses are symbolized by a cross.)

data were not considered for further analysis. As previously shown by Berche (11), the first bacteremia induced by the i.v. challenge disappears within 6 h after mice injection. As shown in Fig. 1, 6 h after an i.v. injection of 5×10^5 bacteria, placental infection was detectable in the absence of bacteremia. The results suggest that, in contrast to the brain (11), infection of the placenta occurs immediately after the initial bacteremia caused by i.v. injection of free bacteria. With lower doses, infection of the placenta could not be detected until later time points, probably due to relatively low sensitivity of the assay, which we estimated can detect around 10 bacteria per placenta. By day 1 postinfection, all animals exhibited at least one infected placenta, whatever the bacterial challenge. By days 2 and 3 postinfection, the number of bacteria rapidly increased in the placenta by almost 2 log units per day. At that time, the secondary bacteremia induced by bacterial growth in infected organs (liver and spleen) may contribute to the infection of the placenta. This rapid growth contrasts with that observed in the liver and spleen, where bacterial growth was diminished by days 2 to 3 of infection. The percentage of infected placentas was dependent upon the inoculum (Fig. 1B, right panel). Challenge with 5×10^5 bacteria induced infection of 100% of placentas and fetuses by day 2, and 50% of mice experienced spontaneous abortions by day 3. With 5×10^3 bacteria, the initial bacterial load of placenta was relatively low but reached a mean of about 1×10^3 bacteria/placenta by day 3. For this inoculum, only 67% of placenta and corresponding fetuses were infected, and about 50% of infected mice could give birth to healthy premature neonates by 18 to 19 days of gestation. The surviving mothers and neonates were followed for 2 months. These mice did not show any symptoms of listeriosis (data not shown). We observed that infection of placenta is absolutely required for fetal infection. Indeed, we never observed any fetal infection associated with a noninfected placenta, suggesting that the crossing of the placental barrier depends upon the bacterial load of the placenta. In addition we observed that, in the uterine corns of the same mouse, a placenta infected with up to 1×10^5 bacteria could be surrounded by noninfected placentas, clearly demonstrating that placental infection is independent of neighboring placentas. Finally, we statistically determined that the higher probability of fetal infection is associated with the bacterial load of the placenta. By using all data obtained with 185 feto-placental units, the respective cutoff values were calculated between 1.0×10^3 and 2.1×10^3 bacteria/placenta (Table 1), confirming that fetal infection requires previous bacterial growth in the placenta.

TABLE 1. Prediction of fetal infection and bacterial placental load[a]

Injected inoculum (CFU)	FPU (*n*)	Cutoff (CFU)	% Se	% Sp	% NPV	% PPV
5×10^3	51	1.7×10^3	87.5	93	97.6	70
5×10^4	58	2.1×10^3	100	85.7	100	82.1
5×10^5	76	1×10^3	100	86	100	84.6
Total	185	1.7×10^3	98.4	88.4	99.1	81.8

[a] Cutoff values correspond to level of bacterial load giving the highest probability for fetal infection. FPU, feto-placental units; Se, sensitivity; Sp, specificity; NPV, negative predictive value; PPV, positive predictive value. Total corresponds to the pooled data independently of the inoculum size.

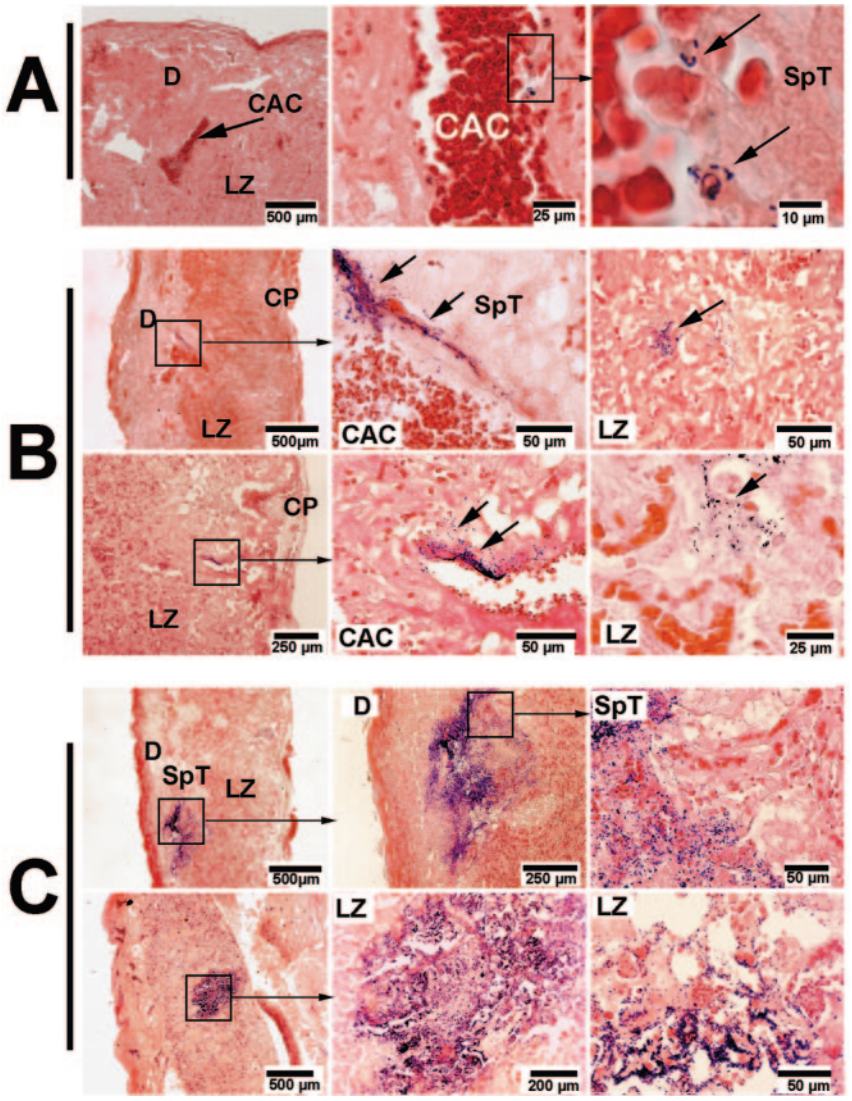

FIG. 2. Anatomical progression of the murine placental infection by *L. monocytogenes*. Gram-Weigert staining at different magnifications performed on placental sections (A) 24 h, (B) 48 h, and (C) 72 h after intravenous infection with 2×10^5 *L. monocytogenes*. Arrows indicate the infective foci. A. Adhesion and internalization of *L. monocytogenes* on the central arterial canal (CAC) wall of placenta infected with 3 log CFU/organ 24 h after infection. B. Evolution and spreading of initial infective foci in the adjacent structures of proximal (top panels) and distal (lower panels) central arterial canals (CAC) and bacterial foci in the labyrinthine zone (LZ) of placenta infected with 6 log CFU/organ 48 h after infection. C. Late progression of placental infection of infective foci in maternal decidua basalis (D), spongiotrophobast (SpT), and labyrinthine zone (LZ) of placenta loaded with 8 log CFU/organ 72 h after infection. CP, chorionic plate.

Our results indicate that the infection of placenta occurs early after the initial bacteremia induced by i.v. inoculation and is not simply a consequence of an uncontrolled infection of liver and spleen.

Early invasion of placenta by *L. monocytogenes*. We then studied the anatomical progression of *L. monocytogenes* within the placental structures (decidua basalis, central arterial canal, spongiotrophoblast, and labyrinthine zone). Infected placentas were collected 1 to 3 days after i.v. infection with 2×10^5 bacteria. Placental disks were divided into two parts, one for bacterial counts, the other for quantitative histological studies. Serial sections were then studied after Gram-Weigert and hematoxylin-eosin stains, and slides were systematically analyzed in a double-blind fashion for each anatomical structure of the placenta (Fig. 2). On average, 6 to 10 serial sections were analyzed per placenta. By day 1 postinfection, bacteria were mainly visualized along the central arterial canal, either free in blood circulation, adhering to the vascular wall of the central arterial canal, or internalized within the cells layering the vessel wall (Fig. 2A). In the labyrinthine zone of examined placentas, we observed very rare bacteria either isolated or localized in small foci (Table 2). By that time, we did not observe inflammatory foci in any of the examined anatomical structures of the placenta and no bacteria were seen in the decidua basalis, probably due to the low sensitivity of the histological approach compared to bacterial quantification (Table 2). By day 2 postinfection, the placentas analyzed by histology contained 1×10^3 to 1×10^5 CFU/placenta. Bacteria were ob-

TABLE 2. Anatomical progression of *L. monocytogenes* placental infection[a]

Time (h)	Sections/ placentas	No. of *L. monocytogenes* foci in:			
		DB	SpT	LZ	CAC[b]
24	48/6	0	0	1	3 (10)
48	124/14	0	6	12	12 (28)
72	216/24	18	30	66	36 (48)

[a] For each indicated time, the placentas were collected from 6 mice infected with 2×10^5 *L. monocytogenes* organisms and analyzed for the number of bacterial foci (about 10 bacteria/focus) for each anatomical structure of the placenta. CAC, central arterial canal; DB, decidua basalis; LZ, labyrinthine zone; SpT, spongiotrophoblast. Sections/placentas indicates the number of sections analyzed and obtained from *n* different placentas.

[b] The number in parentheses corresponds to the number of sections analyzed which showed a CAC structure.

served both in the proximal and distal part of the central arterial canal, adhering to and growing within the cells layering the vessel wall, thus constituting rapidly spreading foci (Fig. 2B). Subsequently, bacteria were detected within the adjacent spongiotrophoblast and trophoblastic giant cells surrounding the central arterial canal (Fig. 2B) and ultimately within the labyrinthine area (Table 2). At that time most bacteria were intracellular, but extracellular bacteria were also frequently observed within the lumen of the central arterial canal. This suggests that the release of *L. monocytogenes* from the trophoblastic cell wall into the maternal circulation might provide a continuous flow of bacteria towards the labyrinthine zone, thus continuously exposing the cells of the villous axis of the labyrinthine zone to infection. These cells form the feto-placental barrier, separating both maternal and fetal circulation, and allow only selective exchanges. As shown in Fig. 2B and Table 2, bacterial foci clearly appear at this time inside the villous. By day 3 postinfection, the number of infective foci was further increased. As shown in Table 2, a dramatic spreading of infection to all the anatomical structures of placenta is observed by day 3, particularly to the labyrinthine zone and to the maternal decidua basalis, where foci rapidly expand (Fig. 2C). Altogether these results suggest that bacteria predominantly adhere to, are internalized by, and grow within most differentiated placental trophoblastic cells.

Trophoblastic cells are the early targets of *L. monocytogenes*. The perfusion of placenta is characterized by high-flow and low-resistance circulation. This is achieved by spiral arteries penetrating the myometrium. It has been recently demonstrated in mice that the endothelial cells lining the lumen of these vessels are replaced by fetal trophoblastic cells when maternal vessels reach the decidua basalis (4). This is also associated with a complete loss of organized smooth muscle actin surrounding the vessel. To identify trophoblastic tissue within the placenta structures, we examined cytokeratin staining on histological sections of placentas 2 days after the infection with 1×10^5 bacteria. We observed that trophoblastic cells lining the lumen of vessels penetrating the decidua basalis correspond to the zone where *L. monocytogenes* is first detected (Fig. 3A). In the labyrinthine zone, the feto-placental barrier is visualized by anti-cytokeratin staining, showing that each villosity is lined by a layer of trophoblastic cells (syncytiotrophoblastic and cytotrophoblastic cells) (Fig. 3B, panels 1 and 2). Endothelial cells of fetal capillaries are easily distin-

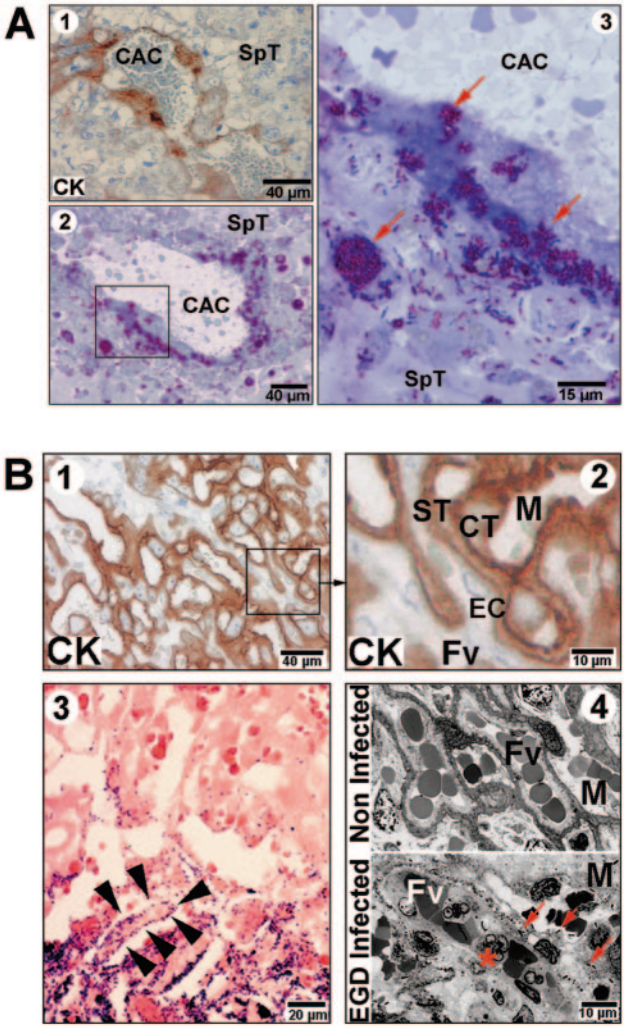

FIG. 3. *L. monocytogenes* is internalized in murine placental trophoblastic cells. The placentas of pregnant mice infected with 2×10^5 *L. monocytogenes* were prepared 48 h after the i.v. injection and analyzed by immunostaining with cytokeratin, Gram-Weigert staining, and semithin sections. A. Endovascular trophoblast cells lining the central arterial channel (CAC) are infected by *L. monocytogenes*: panel 1, immunostaining with cytokeratin (CK); panels 2 and 3, semithin sections. Bacteria are localized within the trophoblastic cells (panels 2 and 3) of the CAC wall and spread to the adjacent trophoblastic giant cells of murine spongiotrophoblast (SpT). B. *L. monocytogenes* infects villous trophoblastic cells of the labyrinthine zone. Cytokeratin immunostaining (CK) (panels 1 and 2) of placental labyrinthine zone identified the trophoblastic cells (ST, syncytiotrophoblast; CT, cytotrophoblast) surrounding the fetal villosity. Trophoblastic cells are exposed to the maternal (M) circulation in contrast with fetal vessels (Fv), which are separated from the trophoblastic cells by a cytokeratin-negative cell monolayer corresponding to fetal endothelial cells (EC) (panel 3). The Gram-Weigert staining of infected placenta indicate that the bacteria massively infect the trophoblastic cells lining the villosities and spread horizontally through the trophoblastic cell layer (delimited by arrowheads) (panel 4). Semithin sections of the labyrinthine zone of noninfected (top panel) and infected placenta (lower panel). Red arrowheads indicate intracellular bacteria, and an asterisk indicates PMN leukocytes inside the fetal vessel (Fv).

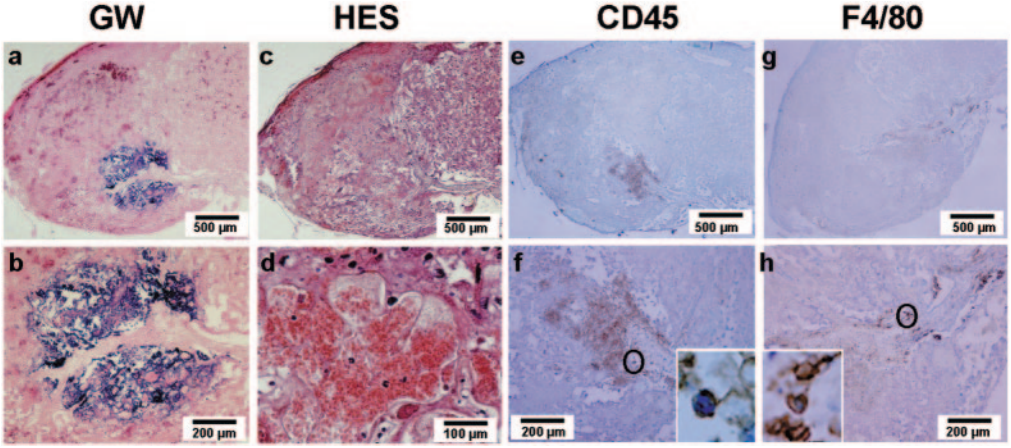

FIG. 4. Vascular and inflammatory consequences of *L. monocytogenes* infection of the labyrinthine zone. Placenta of pregnant mice collected 72 h after infection by 2×10^5 CFU of *L. monocytogenes* (bacterial load of the placenta was 8 log CFU). Infectious foci are visualized with Gram-Weigert stains (GW) (a and b) and the vascular consequences by hematoxylin-eosin stains (HES) (c and d). The inflammatory reaction was observed on sections of placenta stained with the anti-common leukocyte (CD45) (e and f) and the anti-F4/80 antibodies (g and h) to visualize leukocytes and macrophages, respectively. Magnifications (×1,000) show the general morphology of the respectively labeled cells (f and h).

guished, because they are not stained by anti-cytokeratin antibody (Fig. 3B, panels 1 and 2). The trophoblastic cells lining the villosities are often massively infected by *L. monocytogenes* (Fig. 3B, panels 3 and 4). Inside these trophoblastic cells, bacteria can grow and spread all over the syncytiotrophoblastic cells covering the villous axis. Altogether our results demonstrate that (i) the trophoblastic cells lining the central arterial canal (endovascular trophoblast) are the first cells of placenta targeted by *L. monocytogenes* in vivo; and (ii) bacteria invade and grow within the villous trophoblastic cells of the feto-placental barrier, suggesting that the vertical infection of the fetus may occur by cell-to-cell spreading.

The role of polymorphonuclear cells in the placenta barrier. We previously found that almost 50% of pregnant mice infected with 5×10^3 bacteria (the lower inoculum) survived and produced healthy preterm birth. This suggests that, in pregnant mice, an anti-*Listeria* defense could exist to control bacterial growth in the placenta after day 2 of infection. This could occur through an inflammatory reaction in the placenta, which might be important to consider in the early placental invasion by *L. monocytogenes*. To address this question, placentas were collected from pregnant mice sacrificed 3 days after i.v. infection with 2×10^5 bacteria. We separated placentas into two parts to evaluate bacterial loads and to perform histological studies. Serial sections were examined after Gram-Weigert and hematoxylin-eosin stains or after immunostaining with CD45 and F4/80 monoclonal antibodies (Fig. 4). Gram-Weigert staining revealed large bacterial foci within the labyrinthine zone surrounding fetal vessels (Fig. 4a and b). Histological analysis by hematoxylin-eosin staining revealed a basophilic material corresponding to bacterial growth all over the frame associated with central necrosis encircled by fibrin coagulation. The tissue organization was preserved within the infectious foci, suggesting a mechanism of fetal ischemia to explain the central necrosis due to a peripheral blood stasis in the intervilli spaces (Fig. 4d). Along the fetal vascular axis, we observed a proliferating inflammatory reaction where PMNs predominated. The area of inflammation were demarcated by CD45-positive staining (Fig. 4e) with most CD45-positive cells displaying a PMN morphology (Fig. 4f). Immunostaining using the F4/80 antibody clearly shows that leukocyte infiltration of the infected foci taking place in the labyrinthine zone is not predominated by macrophages. These results indicate that the induction of a powerful inflammatory reaction in the heavily infected placenta, mostly consisting of PMNs, might participate in the anti-*Listeria* defense.

To further study the requirement for PMNs in the innate placental host response against *L. monocytogenes* and the subsequent fetal infection, we injected pregnant mice with the MAb RB6-8C5, known to selectively deplete mature PMNs and eosinophils (45). The efficacy of this MAb for depleting PMNs was first assessed by examining its effect in the blood leukocyte count of pregnant mice 24 h after the injection and comparing that to control pregnant mice treated with rat IgG. As previously described for nonpregnant mice, the treatment of pregnant mice with MAb RB6-8C5 induced more than 90% depletion of blood PMNs, while monocyte and lymphocyte counts were not significantly modified (Table 3). We further analyzed, by flow cytometry, the efficiency of this MAb for depleting RB6-8C5 and Ly6G-1A8 cells (almost all PMNs) among leukocyte ($CD45^+$) populations. This was studied in hematopoietic organs of mothers (bone marrow) and of fetuses (fetal liver). As shown in Fig. 5, the treatment with MAb

TABLE 3. Effect of RB6-8C5 MAb treatment on blood leukocytes of noninfected pregnant mice[a]

Treatment	Total leukocyte (per mm^3 blood ± SD)	% PMN	% Lymphocyte	% Monocyte
Control	4,070 ± 1,274	12.1 ± 6.1	80.2 ± 7.4	2.4 ± 0.8
RB6-8C5	1,656 ± 1,190	0.3 ± 0.5	97.6 ± 1.5	2 ± 1

[a] Cellular counts were determined by Coulter 24 h after RB6-8C5 treatment in noninfected mice. For RB6-8C5 treatment, mice were injected with 250 μg of RB6-8C5. Control mice were injected with 250 μg of rat IgG. PMN, polymorphonuclear cells ($n = 5$ per group).

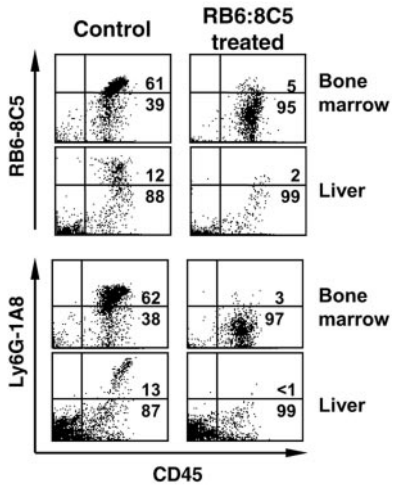

FIG. 5. Flow cytometric analysis of noninfected maternal bone marrow cells and fetal liver leukocytes 24 h after RB6-8C5 MAb treatment. The combined expression of $CD45^+$:RB6-8C5$^+$ and $CD45^+$:Ly6G-1A8$^+$ was compared to that of pregnant control mice injected with 0.25 mg of rat IgG. The percentages given for each scatter are determined within the $CD45^+$ cell population. Data shown are from one of three experiments giving equivalent results.

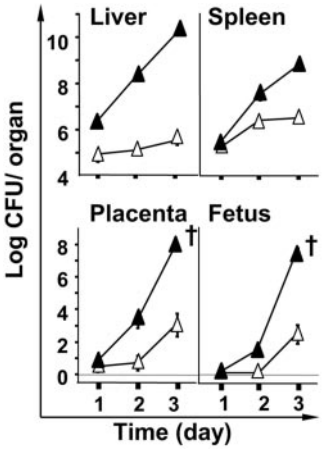

FIG. 6. Effect of the depletion of polymorphonuclear cells on *L. monocytogenes* growth in pregnant mice infected intravenously with 5×10^3 bacteria. Mice treated with RB6-8C5 MAb (filled triangles) were compared to nontreated pregnant control mice (open triangle). Bacterial growth was quantified for each organ (liver and spleen) and placenta or fetus at the indicated time. Results shown are the means ± standard errors from groups of 3 mice and are expressed as $\log_{10}$ CFU per organ. Average litter size, 5.9 ± 1.3 placenta; range, 3 to 7. Error bars, not visible, are smaller than the symbols. By performing two-factor analysis of variance, the comparisons of bacterial growth between RB6-8C5-treated and nontreated pregnant control mice were statistically significant ($P < 0.0001$) for all studied organs. (Fetal losses are symbolized by a cross.)

RB6-8C5 strongly depletes PMN from both mothers and fetuses. We then studied the consequences of PMN depletion in pregnant mice infected with 5×10^3 CFU of *L. monocytogenes*. Mice were sacrificed 1 to 3 days after the inoculation and bacterial counts were determined in the liver, the spleen, and for each placenta and fetus. At day 1, we observed a significant increase of the bacterial load in the liver but not in the spleen of PMN-depleted mice compared to nontreated controls (Fig. 6). By days 2 to 3 postinfection, the exacerbation of infection remained more dramatic in the liver than in the spleen, reaching very high levels in these organs in depleted mice (1×10^8 to 1×10^{10} bacteria per organ). By day 3, bacterial counts were as much as 4 to 5 logs higher in PMN-depleted mice than in nontreated controls (Fig. 6). These results are consistent with previous studies performed in nonpregnant mice (13, 40), showing that PMNs are more involved in anti-listerial defense in the liver than in the spleen (13). Interestingly, by day 1 postinfection there was no difference in terms of bacterial growth in the placenta of RB6-8C5-treated mice compared to those of control mice, and the fetuses remained uninfected. By days 2 to 3 postinfection, we observed a dramatic increase of bacterial growth in the placentas and fetuses of depleted pregnant mice compared to controls. The massive infection of placenta was almost always associated with fetal infection by days 2 to 3, whereas the fetuses of the control group remained uninfected or weakly infected. By using the data obtained with the infective doses of 5×10^3 bacteria in depleted mice, we could calculate the cutoff values corresponding to the placental bacterial load associated with the higher probability for fetal infection. The cutoff value was estimated at 1.7×10^3 bacteria per placenta, a value similar to that determined for control mice infected up to 5×10^5 bacteria (Table 1). Altogether, these results clearly indicate that, when placenta is invaded by *L. monocytogenes*, PMNs are not involved in its defense during the early stage of infection. Rather, PMNs play a major role in the defense of the placenta against bacterial invasion by controlling the bacterial spreading and the subsequent fetal infection after the disruption of the feto-placental barrier.

DISCUSSION

Although listeriosis occurs under natural conditions after ingestion of contaminated food, it is difficult to reproduce placental infection in mice by the oral route, because few *L. monocytogenes* organisms cross the intestinal barrier, even in mice infected with very high doses of bacteria (17, 21, 26, 29). However, we performed preliminary experiments confirming that the placental invasion occurs in orally infected mice, but the infection is weakly reproducible (data not shown). For this reason, we used the previously described intravenous infection route to study the feto-placental invasion, which gives reproducible results in the model of murine listeriosis (2, 30, 38, 39). The duration of gestation in mice is between 19 and 21 days. In our model, pregnant BALB/c mice were infected at day 14, corresponding to the last period of gestation. At that time, the vascularization of placenta is complete in mice (4, 15, 41), which is the most convenient time to study feto-maternal transmission of *L. monocytogenes*, as previously reported (2). In accordance with the results published by Redline and Lu, we found that gestation did not induce any increase of systemic susceptibility to listeriosis, since bacterial growth in organs was easily controlled for low doses in pregnant mice, as it was in nonpregnant mice (37). However, the placenta is exquisitely susceptible to bacterial invasion, since doses as low as 1×10^3 bacteria, inoculated i.v., were sufficient to induce feto-placental infection and bacterial growth.

Bacteria were detected as early as 6 h postinfection, suggesting that the inoculation of placenta occurs almost immediately after inducing the initial bacteremia. Indeed, it is known that free bacteria inoculated i.v. disappear within a few minutes with low doses (11). This means that the initial free circulating bacteria can therefore invade the placenta at the very early phase of infection. Our data are in agreement with a previous report suggesting that infection of placenta does not result from heavily infected spleens and livers, which induce a secondary bacteremia after 1 to 2 days following the initial i.v. challenge (38). In contrast, invasion of the brain occurs during murine listeriosis as a consequence of a secondary bacteremia originated from heavily infected foci of the bone marrow and organs (11, 23, 32, 34). After this early invasion of the placenta, bacterial growth was extremely rapid in placentas and fetuses. This uncontrolled growth can be explained by a weak antilisterial response within the placenta related to the local immunosuppression that prevents maternal anti-fetal response (37). Bacteria grew independently in each placenta regardless of bacterial growth in other placentas or organs. Interestingly, in the uterine corns of the same mother, a placenta infected with more than 1×10^5 bacteria per placenta can be surrounded by sterile placentas. After 72 h, bacterial loads in placentas were less dispersed than in the first 48 h, suggesting that placental infection may be boosted by the secondary bacteremia originated from heavily infected organs (liver, spleen, bone marrow, and other placentas).

Placental infection always preceded fetal infection. As expected and previously demonstrated, we found that *L. monocytogenes* infects the trophoblast, a tissue consisting of fetally derived epithelial cells which forms a physical barrier between the maternal and the fetal circulations. By histological study, we found that endovascular, villous, and extravillous trophoblast cells could be infected by *L. monocytogenes*. These data are consistent with recent published reports showing that bacteria invade trophoblast cells from human placenta (28) and human placental cell lines in vitro (6). That bacteria can be internalized by trophoblastic cells is not surprising, since these cells share many similarities with macrophages, including phagocytosis, syncytialization, invasiveness, and expression of many proteins and cytokine receptors (5, 19, 41). Moreover, it is known that, in mature placentas, trophoblast cells participate in fetal innate immune defense through the elimination of microorganisms present in the blood circulation (5). In keeping with this, it has been recently published that internalization of bacteria in trophoblast cell lines requires the expression of internalin (InlA) (28), a surface-exposed bacterial protein that binds with high affinity to human E-cadherin (14). Since guinea pig E-cadherin binds to internalin with the same affinity as that of humans, the guinea pig model might be ideal to explore the role of interaction between InlA and E-cadherin in the placenta invasion by *L. monocytogenes*. Surprisingly, no difference in fetal infection was found between wild-type bacteria and InlA-deleted mutants in guinea pigs (6), suggesting that other mechanisms may contribute to the bacterial internalization into the trophoblast cells.

A precise histological study allowed us to follow the kinetics of placental invasion during listeriosis. We found that the lumen of central arterial canals is lined by fetal trophoblastic cells that stain with anti-cytokeratin antibodies, thus confirming recent results showing that trophoblastic cells progressively replace endothelial cells in these canals (4). Our main finding was that these endovascular trophoblastic cells were the first infected cells in the placenta. This most likely occurs immediately after i.v. inoculation. Endothelial cells of spiral arteries switch to endovascular trophoblasts at the level of the distal decidua basalis (4). Indeed, the earliest infectious foci visible in the placenta were located in trophoblast cells of the central arterial canals walls, loaded with intracellular bacteria and preceding the bacterial invasion of the adjacent decidua basalis (Fig. 7). This is in contrast with a previous report suggesting that the first site of infection is the decidua basalis (38). We observed that bacteria sequentially spread to other trophoblastic structures, the decidua basalis, and the labyrinthine zone, where the syncytiotrophoblast bilayers of villi constitute the anatomical and biological barrier between fetal and maternal blood encompassing the fetal capillaries (Fig. 7) (27). Therefore, our data indicate that bacteria grow in the syncytiotrophoblast before crossing the placental barrier to ultimately infect the fetus. Moreover, the crossing might occur by bacterial cell-to-cell spreading through the trophoblastic tissues, ultimately reaching the fetal capillaries. This hypothesis is supported by recent findings in a guinea pig model, demonstrating that the expression of ActA by the bacteria is required for the crossing of the feto-placental barrier (7).

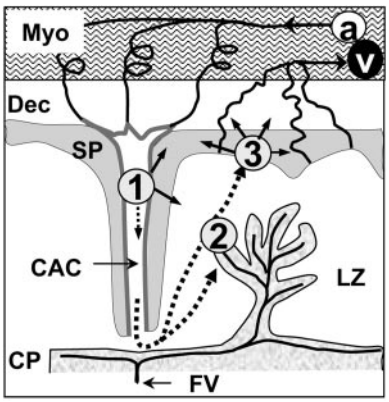

FIG. 7. Progression of the placental invasion by *L. monocytogenes*. *L. monocytogenes* first infects the endovascular trophoblast (1) and diffuses to the adjacent spongiotrophoblast or through maternal blood circulation to the syncytiotrophoblast of the labyrinthine zone (2) or other nonvillous trophoblastic structures (3). a, maternal spiral arteries; CAC, central arterial channel; CP, chorionic plate; Dec, decidua basalis; FV, fetal vessels; LZ, labyrintine zone; Myo, myometer; SP, songiotrophoblast; v, maternal venous circulation.

The progression of placental invasion can be explained by the development of the mouse placenta. The blood circulation of human and murine placentas share many similarities (41). In both species, maternal blood emerges from spiral arteries into intervillous spaces surrounding the highly branched villous complexes of the labyrinthine area. However, entry of blood into the intervillous space is slightly different between the two species. In the murine placenta, the supply arteries branch into several spiral-shaped arteries, cross the decidua basalis, and converge towards the trophoblast giant cell layer to form a small number (1 to 4) of central arterial canals (4). Hence, maternal blood, brought by few central arterial canals, is directed to the

chorionic plate (4, 42). It is not known how *L. monocytogenes* infection progresses in human placenta. In view of our results, we suggest that in humans the infection also can be initiated in the endovascular trophoblast lining spiral arteries which cross the decidua basalis just before projecting the maternal blood in the intervillous spaces. In contrast to mouse circulation, no canal-like structures have been described in humans, but it is widely accepted that endovascular trophoblasts may invade as far as the myometrium vessels in humans (36).

The immunological status of the placenta is remarkable and characterized by a predominant Th_2-anti-inflammatory response required to prevent the rejection of the fetus. In noninfected placenta, there is no recruitment of PMNs and macrophages in the labyrinthine zone, since adhesion molecules, such as intracellular adhesion molecule (ICAM), are not expressed at basal levels in trophoblastic cells (47). During listeriosis in pregnant mice, we found that an inflammatory reaction predominantly consisting of PMNs occurs in infected placentas, thus suggesting that these cells might participate in the control of the placental infection. In contrast to a previous study showing an inflammatory response mostly localized to the decidual area, we also observed that the inflammatory response to bacteria was diffuse within the labyrinthine zone and the villi. Our results corroborate those of Redline and Lu, who found an inflammatory reaction in the labyrinthine zone after an i.v. inoculum of 2×10^5 CFU (37). The cellular composition of inflammatory listerial lesion in the decidual area and in the labyrinthine zone mainly consists of PMNs (37). Herein we found that, 72 h postinfection, the recruited PMNs in the labyrinthine zone followed the axis of fetal large vessels from the placenta. This suggests that PMNs in the labyrinthine zone may also originate from fetal circulation. This notion is also supported by the presence of mobilized PMNs trapped in infected villi (Fig. 3B, panel 4). We then examined the role of PMNs in the placental barrier by treating pregnant mice with the IgG MAb RB6-8C5. Bacterial growth dramatically increased in trophoblastic cells, becoming almost uncontrolled in the placentas and fetuses of depleted mice. Since the placental barrier is permeable to IgG immunoglobulin, the MAb also depletes fetal leukocytes. These results in the placenta are very similar to those observed in the spleen and liver of PMN-depleted nonpregnant mice infected by *L. monocytogenes* (13, 16, 40). As suggested for the liver (13), PMNs might adhere to and lyse infected trophoblastic cells, thus exposing extracellular bacteria to PMNs. The accumulation of PMNs in the placenta might be due to the activation of the syncytiotrophoblast cells by proinflammatory cytokines enhancing the expression of ICAM-1, thus facilitating the local adhesion and accumulation of PMNs (47). Our results also corroborate a recent study demonstrating that placenta is responsive to CSF-1, which regulates the synthesis, by the trophoblast, of the PMN chemoattractants KC and MIP-2 in response to *Listeria* infection during pregnancy (20). CSF-1 is synthesized in the utero-placental unit, and its receptor is expressed on trophoblastic cells in mammalian species. Thus, the CSF-1 pathway and the subsequent PMN recruitment is considered to be a central component of the placental innate immune response to *Listeria* infection (20). In the late infection of placenta by *L. monocytogenes*, we observed important modifications of the placental circulation associated with the inflammatory response. As a consequence of massive infection of the labyrinthine zone, fetal vessels undergo thrombosis provoking ischemic central necrosis. The thrombosis may be initiated by the local inflammation that stimulates endothelial tissue factor-mediated procoagulant activity in the fetal endothelium. These circulatory disorders with fetal thrombosis may participate in spontaneous abortion protecting the mother and eventually the fetus.

Altogether, our results demonstrate that the pregnant mouse is a suitable model to study congenital listeriosis and placental invasion by *L. monocytogenes.* Infection of the placenta is dependent upon the early exposition of permissive trophoblastic cells that can be infected with free circulating bacteria. Bacteria are initially trapped in endovascular trophoblastic cells lining the central arterial canals and then progress rapidly to other trophoblastic structures of the placenta. Bacterial growth in the placenta up to a cutoff value of around 1×10^3 CFU/placenta is determinant for the crossing of the feto-placental barrier. Finally, in our model, although neutrophils play an important role in controlling the infection, their depletion does not modify the level of bacterial growth required in the placenta to induce fetal infection.

ACKNOWLEDGMENTS

We are very grateful to Michèle Leborgne and Gérard Pivert for their technical assistance (Medical School Rene Descartes Paris-5) and Darin Fogg for careful reading of the manuscript.

This work was supported by University Rene Descartes-Paris 5, INSERM, and Assistance Publique des Hôpitaux de Paris.

REFERENCES

1. **Abbasi, M., K. Kowalewska-Grochowska, M. A. Bahar, R. T. Kilani, B. Winkler-Lowen, and L. J. Guilbert.** 2003. Infection of placental trophoblasts by *Toxoplasma gondii*. J. Infect. Dis. **188:**608–616.
2. **Abram, M., and M. Doric.** 1997. Primary *Listeria monocytogenes* infection in gestating mice. Folia Microbiol. **42:**65–71.
3. **Abram, M., D. Schluter, D. Vuckovic, B. Wraber, M. Doric, and M. Deckert.** 2003. Murine model of pregnancy-associated *Listeria monocytogenes* infection. FEMS Immunol. Med. Microbiol. **35:**177–182.
4. **Adamson, S. L., Y. Lu, K. J. Whiteley, D. Holmyard, M. Hemberger, C. Pfarrer, and J. C. Cross.** 2002. Interactions between trophoblast cells and the maternal and fetal circulation in the mouse placenta. Dev. Biol. **250:** 358–373.
5. **Amarante-Paffaro, A., G. S. Queiroz, S. T. Correa, B. Spira, and E. Bevilacqua.** 2004. Phagocytosis as a potential mechanism for microbial defense of mouse placental trophoblast cells. Reproduction **128:**207–218.
6. **Bakardjiev, A. I., B. A. Stacy, S. J. Fisher, and D. A. Portnoy.** 2004. Listeriosis in the pregnant guinea pig: a model of vertical transmission. Infect. Immun. **72:**489–497.
7. **Bakardjiev, A. I., B. A. Stacy, and D. A. Portnoy.** 2005. Growth of *Listeria monocytogenes* in the guinea pig placenta and role of cell-to-cell spread in fetal infection. J. Infect. Dis. **191:**1889–1897.
8. **Barragan, A., and L. D. Sibley.** 2003. Migration of *Toxoplasma gondii* across biological barriers. Trends Microbiol. **11:**426–430.
9. **Benirschke, K.** 1998. Remarkable placenta. Clin. Anat. **11:**194–205.
10. **Benshushan, A., A. Tsafrir, R. Arbel, G. Rahav, I. Ariel, and N. Rojansky.** 2002. *Listeria* infection during pregnancy: a 10 year experience. Isr. Med. Assoc. J. **4:**776–780.
11. **Berche, P.** 1995. Bacteremia is required for invasion of the murine central nervous system by *Listeria monocytogenes*. Microb. Pathog. **18:**323–336.
12. **Buendia, A. J., R. M. De Oca, J. A. Navarro, J. Sanchez, F. Cuello, and J. Salinas.** 1999. Role of polymorphonuclear neutrophils in a murine model of *Chlamydia psittaci*-induced abortion. Infect. Immun. **67:**2110–2116.
13. **Conlan, J. W., and R. J. North.** 1994. Neutrophils are essential for early anti-*Listeria* defense in the liver, but not in the spleen or peritoneal cavity, as revealed by a granulocyte-depleting monoclonal antibody. J. Exp. Med. **179:** 259–268.
14. **Cossart, P., and M. Lecuit.** 1998. Interactions of *Listeria monocytogenes* with mammalian cells during entry and actin-based movement: bacterial factors, cellular ligands and signaling. EMBO J. **17:**3797–3806.
15. **Cross, J. C., M. Hemberger, Y. Lu, T. Nozaki, K. Whiteley, M. Masutani, and**

S. L. Adamson. 2002. Trophoblast functions, angiogenesis and remodeling of the maternal vasculature in the placenta. Mol. Cell Endocrinol. **187:**207–212.
16. **Czuprynski, C. J., J. F. Brown, N. Maroushek, R. D. Wagner, and H. Steinberg.** 1994. Administration of anti-granulocyte MAb RB6-8C5 impairs the resistance of mice to *Listeria monocytogenes* infection. J. Immunol. **152:**1836–1846.
17. **Gaillard, J. L., F. Jaubert, and P. Berche.** 1996. The inlAB locus mediates the entry of *Listeria monocytogenes* into hepatocytes *in vivo*. J. Exp. Med. **183:**359–369.
18. **Gray, M. L., and A. H. Killinger.** 1966. *Listeria monocytogenes* and listeric infections. Bacteriol. Rev. **30:**309–382.
19. **Guilbert, L. J., B. Winkler-Lowen, A. Smith, D. R. Branch, and M. Garcia-Lloret.** 1993. Analysis of the synergistic stimulation of mouse macrophage proliferation by macrophage colony-stimulating factor (CSF-1) and tumor necrosis factor alpha (TNF-alpha). J. Leukoc. Biol. **54:**65–72.
20. **Guleria, I., and J. W. Pollard.** 2000. The trophoblast is a component of the innate immune system during pregnancy. Nat. Med. **6:**589–593.
21. **Hamrick, T. S., J. R. Horton, P. A. Spears, E. A. Havell, I. W. Smoak, and P. E. Orndorff.** 2003. Influence of pregnancy on the pathogenesis of listeriosis in mice inoculated intragastrically. Infect. Immun. **71:**5202–5209.
22. **Hyde, S. R., and K. Benirschke.** 1997. Gestational psittacosis: case report and literature review. Mod. Pathol. **10:**602–607.
23. **Join-Lambert, O. F., S. Ezine, A. Le Monnier, F. Jaubert, M. Okabe, P. Berche, and S. Kayal.** 2005. *Listeria monocytogenes*-infected bone marrow myeloid cells promote bacterial invasion of the central nervous system. Cell Microbiol. **7:**167–180.
24. **Kirby, D. R., and S. Bradbury.** 1965. The hemo-chorial mouse placenta. Anat. Rec. **152:**279–281.
25. **Koi, H., J. Zhang, and S. Parry.** 2001. The mechanisms of placental viral infection. Ann. N. Y. Acad. Sci. **943:**148–156.
26. **Lammerding, A. M., K. A. Glass, A. Gendron-Fitzpatrick, and M. P. Doyle.** 1992. Determination of virulence of different strains of *Listeria monocytogenes* and *Listeria innocua* by oral inoculation of pregnant mice. Appl. Environ. Microbiol. **58:**3991–4000.
27. **Leach, L., M. J. Lammiman, M. O. Babawale, S. A. Hobson, B. Bromilou, S. Lovat, and M. J. Simmonds.** 2000. Molecular organization of tight and adherens junctions in the human placental vascular tree. Placenta **21:**547–557.
28. **Lecuit, M., D. M. Nelson, S. D. Smith, H. Khun, M. Huerre, M. C. Vacher-Lavenu, J. I. Gordon, and P. Cossart.** 2004. Targeting and crossing of the human maternofetal barrier by *Listeria monocytogenes*: role of internalin interaction with trophoblast E-cadherin. Proc. Natl. Acad. Sci. USA **101:**6152–6157.
29. **Lecuit, M., S. Vandormael-Pournin, J. Lefort, M. Huerre, P. Gounon, C. Dupuy, C. Babinet, and P. Cossart.** 2001. A transgenic model for listeriosis: role of internalin in crossing the intestinal barrier. Science **292:**1722–1725.
30. **Lu, C. Y., R. W. Redline, C. M. Shea, L. B. Dustin, and D. B. McKay.** 1989. Pregnancy as a natural model of allograft tolerance. Interactions between adherent macrophages and trophoblast populations. Transplantation **48:**848–855.
31. **Luft, B. J., and J. S. Remington.** 1982. Effect of pregnancy on resistance to *Listeria monocytogenes* and *Toxoplasma gondii* infections in mice. Infect. Immun. **38:**1164–1171.
32. **Mackaness, G. B.** 1962. Cellular resistance to infection. J. Exp. Med. **116:**381–406.
33. **Mencikova, E., J. Snirc, D. Gubran, J. Smola, and M. Mara.** 1989. Experimental listeriosis in immunized sheep. Acta Microbiol. Hung. **36:**331–334.
34. **North, R. J.** 1970. The relative importance of blood monocytes and fixed macrophages to the expression of cell-mediated immunity to infection. J. Exp. Med. **132:**521–534.
35. **Pappas, G., N. Akritidis, M. Bosilkovski, and E. Tsianos.** 2005. Brucellosis. N. Engl. J. Med. **352:**2325–2336.
36. **Pijnenborg, R., J. M. Bland, W. B. Robertson, G. Dixon, and I. Brosens.** 1981. The pattern of interstitial trophoblastic invasion of the myometrium in early human pregnancy. Placenta **2:**303–316.
37. **Redline, R. W., and C. Y. Lu.** 1987. Role of local immunosuppression in murine fetoplacental listeriosis. J. Clin. Investig. **79:**1234–1241.
38. **Redline, R. W., and C. Y. Lu.** 1988. Specific defects in the anti-listerial immune response in discrete regions of the murine uterus and placenta account for susceptibility to infection. J. Immunol. **140:**3947–3955.
39. **Redline, R. W., C. M. Shea, V. E. Papaioannou, and C. Y. Lu.** 1988. Defective anti-listerial responses in deciduoma of pseudopregnant mice. Am. J. Pathol. **133:**485–497.
40. **Rogers, H. W., and E. R. Unanue.** 1993. Neutrophils are involved in acute, nonspecific resistance to *Listeria monocytogenes* in mice. Infect. Immun. **61:**5090–5096.
41. **Rossant, J., and J. C. Cross.** 2001. Placental development: lessons from mouse mutants. Nat. Rev. Genet. **2:**538–548.
42. **Salomon, L. J., N. Siauve, D. Balvay, C. A. Cuenod, C. Vayssettes, A. Luciani, G. Frija, Y. Ville, and O. Clement.** 2005. Placental perfusion MR imaging with contrast agents in a mouse model. Radiology **235:**73–80.
43. **Silver, H. M.** 1998. Listeriosis during pregnancy. Obstet. Gynecol. Surv. **53:**737–740.
44. **Stein, A., and D. Raoult.** 1998. Q. fever during pregnancy: a public health problem in southern France. Clin. Infect. Dis. **27:**592–596.
45. **Tepper, R. I., R. L. Coffman, and P. Leder.** 1992. An eosinophil-dependent mechanism for the antitumor effect of interleukin-4. Science **257:**548–551.
46. **Vazquez-Boland, J. A., M. Kuhn, P. Berche, T. Chakraborty, G. Dominguez-Bernal, W. Goebel, B. Gonzlez-Zorn, J. Wehlnd, and J. Kreft.** 2001. *Listeria* pathogenesis and molecular virulence determinants. Clin. Microbiol. Rev. **14:**581–640.
47. **Xiao, J., M. Garcia-Lloret, B. Winkler-Lowen, R. Miller, K. Simpson, and L. J. Guilbert.** 1997. ICAM-1-mediated adhesion of peripheral blood monocytes to the maternal surface of placental syncytiotrophoblasts: implications for placental villitis. Am. J. Pathol. **150:**1845–1860.

Editor: D. L. Burns